Session II

Stratospheric Aerosol Characteristics during the Volcanic Eruptions using the SAGE III/ISS Observations

B.L. Madhavan and M. Venkat Ratnam

3rd June 2024

STIPMEX @ IITM Pune

Motivation

Volcanic eruptions are unpredictable episodic events which alter the stratospheric aerosol loading, composition, chemistry, and radiative forcing

- LiDARs and in-situ techniques are limited by the number of wavelengths.
- OMPS-LP and SAGE III/ISS provide multiwavelength aerosol extinction profiles.
- Occultation instruments provide more accurate information on aerosol extinction coefficient profiles.

No attempts to infer the size distributions (number/volume)

- Modelling the radiative forcing of aerosols
- Evaluate aerosol effects on ozone

Ambae eruption

Ambae (15° S, 167° E)
➔ April & July 2018
➔ VEI ~ 3

April ➔ Southern Hemisphere alone.

Plume from July ➔ Extended both hemispheres through the lower branch of Brewer-Dobson Circulation.

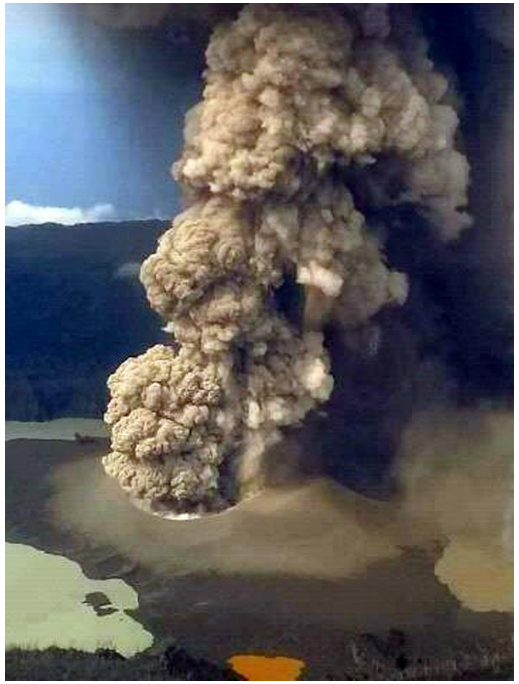

Ambae eruption

Onset of a series of even stronger and record-breaking moderate & large eruptions

- Raikoke (48° N, 153° E; **June 2019**)… VEI ~ 4
- Ulawun (5° S, 151° E; Jun & Aug 2019)… VEI ~ 4
- Hunga Tonga (21° S, 175° E; **Jan 2022**) … VEI ~ 5-6

Data Set & Study Region

SAGE III/ISS
(since June 2017)

384, 449, 521, 602, 676, 756, 869, 1021, and 1544 nm

Assuming a much smaller longitudinal variation for efficient mixing in the zonal direction and strong horizontal transport, latitudinal belts are chosen.

- Northern Hemisphere (NH): 0 to 60° N
- Southern Hemisphere (SH) : 0 to 60° S
- Global : 60° S to 60° N
- 10 to 20° S (Consist Ambae at 15° S)
- 10 to 20° N

Phases/Periods

- Jul 2017
- Mar 2018

Pre-Ambae

- 5 Apr 2018
- 26 Jul 2018

Ambae1

- 27 Jul 2018
- 21 Jun 2019

Ambae2

- 22 Jun 2019
- 31 Jan 2020

Post-Ambae

Canadian wildfires
(Aug 2017 – Jun 2018)

Raikoke
(22 Jun 2019 onwards)

Ulawun
(26Jun 2019 & 3 Aug 2019)

OBJECTIVES

- Inversion method to infer size distributions
- Examine the spatiotemporal variability of stratospheric AOD (sAOD) and size distributions
- Evaluate temporal evolution (growth/decay) characteristics
- Assess the radiative impact of Amabe eruptions

Method

Based on the inversion technique of tropospheric aerosols from the measurements of AOD by a sun photometer (Kudo et al., 2021) and hints from previous methods adopted for SAGE II (Yue, 1999; 2000)

Assumptions

- ❖ **Refractive index of stratospheric sulfate** assumed to be **1.45 – i0** at all wavelengths
- ❖ Number size distribution is assumed to consist of multiple log-normal distributions

$$\frac{dN(r)}{d\ln r} = \sum_{i=1}^{M} N_i \exp\left[-\frac{1}{2}\left(\frac{\ln r - \ln r_{m,i}}{\ln s}\right)^2\right]$$

M – No. of log-normal distributions (same as no. of wavelengths considered)
r – Particle radius (micron)
$r_{m,I}$ – Median (or mode) radius (micron)
s – standard deviation of dN/dlnr function
N_i – Parameter to be retrieved ($\frac{N_0}{\sqrt{2\pi}\ln s}$)

N_o is an integrated value of i^{th} log-normal function.

- ❖ Optical properties of spherical particles are calculated using Mie theory.

Wavelengths taken: 449, 521, 602, 676, 756, 869, 1021, and 1544 nm ➔ **M = 8** (fixed)
Value of s (depends on M) is fixed at **1.221** for each log-normal distribution.
$\mathbf{r_{min} = 0.1}$ **micron,** $\mathbf{r_{max} = 1.0}$ **micron**
$r_{m,i}$ = 0.118, 0.164, 0.228, 0.316, 0.439, 0.611, and 0.848 micron

Parameter N_i is optimized to the measured sAOD with the maximum likelihood method.

Retrieval Assessment

Yue (1999; 2000)

Table 1. Parameters of the six log-normal size distributions of Yue [39,40] used in this study. The first and second columns below the retrieved R_{eff} correspond to sAOD (at 521 nm) = 0.005 and 0.001, respectively. The number of N_i is fixed by 8 in all the retrieval results because the number of the wavelengths is 8.

Model	Type	N_1/N_2	$r_{m,1}$ (μm)	$r_{m,2}$ (μm)	s_1	s_2	Simulated R_{eff} (μm)	Retrieved R_{eff} (μm)	R_{eff} (μm)
A	Monomodal (N_1=N_2)	1.00	0.07	–	1.86	–	0.19	0.22	0.21
B	Monomodal (N_1=N_2)	1.00	0.09	–	1.80	–	0.21	0.23	0.21
C	Bimodal	1.76	0.11	0.43	1.67	1.36	0.50	0.49	0.53
D	Bimodal	1.41	0.11	0.30	1.43	1.48	0.40	0.39	0.38
E	Bimodal	0.98	0.13	0.56	1.58	1.26	0.61	0.62	0.64
F	Bimodal	0.76	0.09	0.39	1.41	1.30	0.45	0.44	0.42

$$R_{eff} = \frac{M_3}{M_2} = 3\left(\frac{V}{S}\right) \qquad \frac{dV(r)}{d\ln r} = V(r)\frac{dN(r)}{d\ln r} = \frac{4}{3}\pi r^3 \frac{dN(r)}{d\ln r}$$

- Retrieved & simulated R_{eff} differ by 0.03 (deviation of $\pm$15%)
- Overestimated fine mode has little influence on R_{eff}
- Size distribution of particles with radius < 0.2 microns was not retrieved accurately.

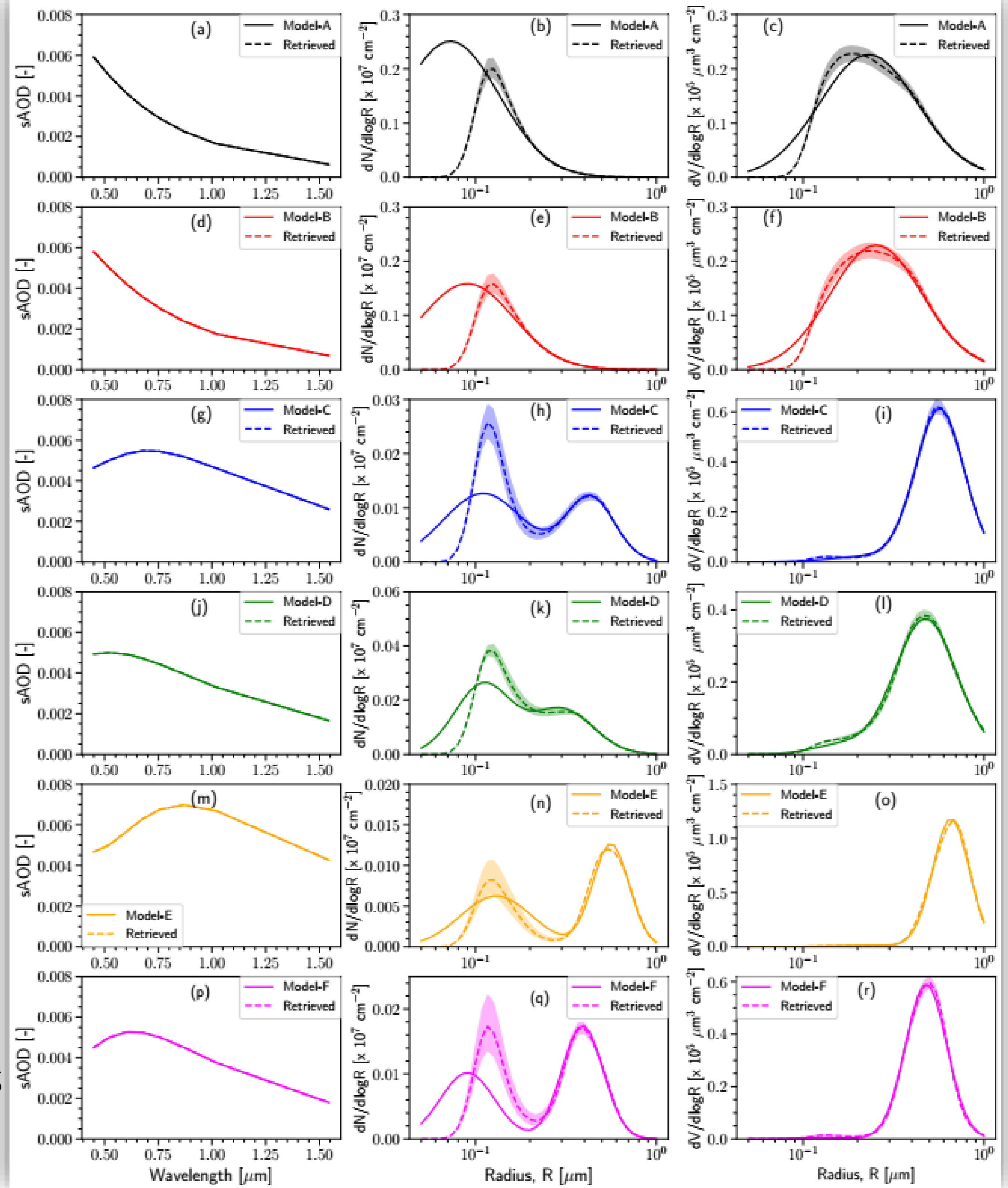

Spatiotemporal variability

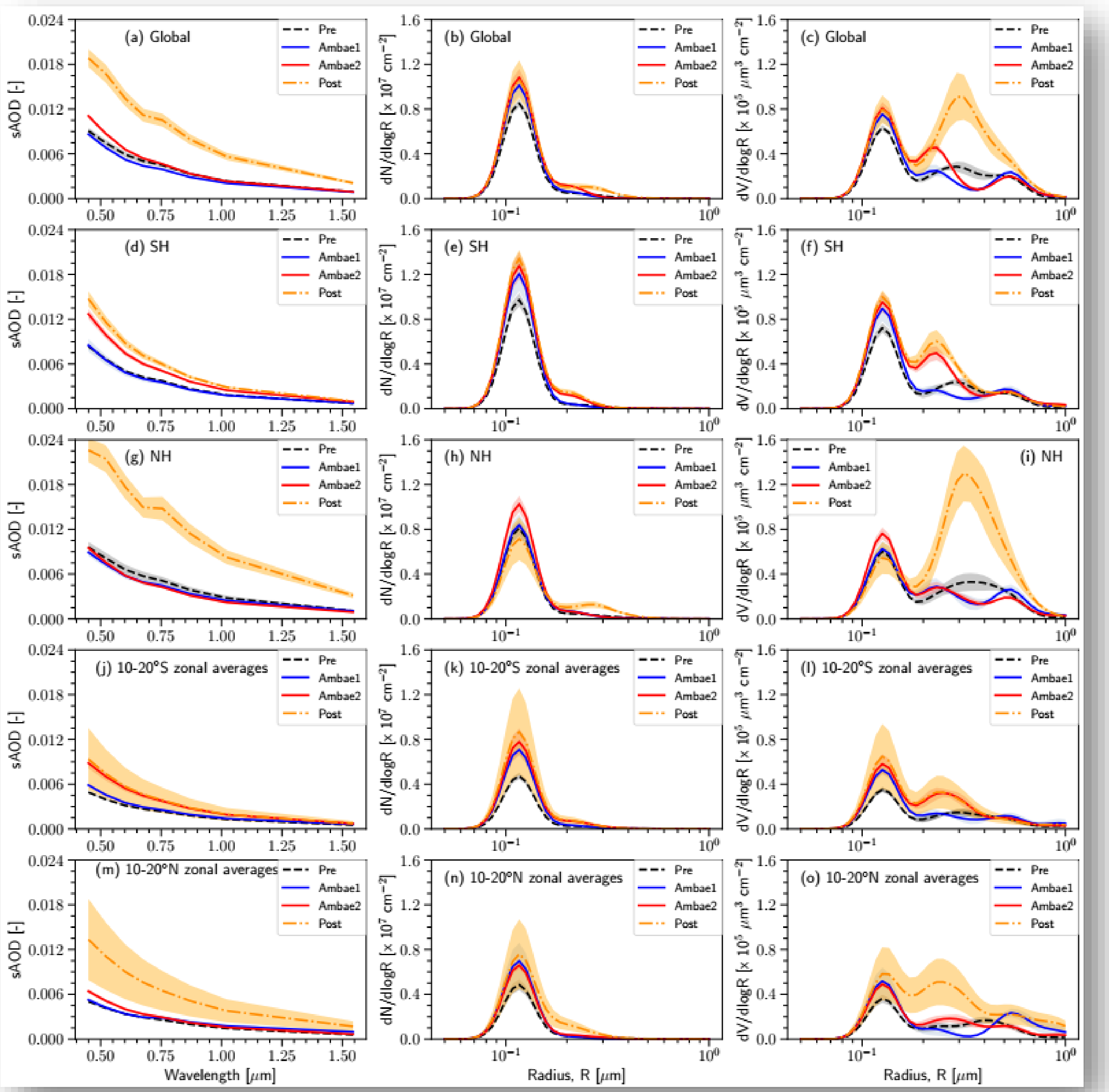

- Distinct spectral behavior of sAOD noticed.
- Monomodal number size distributions appear to be similar, with peaks around 0.12 microns.
- Total number concentrations are different at each region at different periods.
- Bi- and tri-modal volume size distributions are found to vary distinctly.
- Inclusion of higher (1544 nm) and exclusion of smaller (384 nm) wavelengths tends to strongly modify the amplitude of the first principal mode and the shape of the second and third modes.

Dynamical and microphysical processes with varying concentrations & composition in time lead to changes in size distribution.

Growth & Decay Characteristics

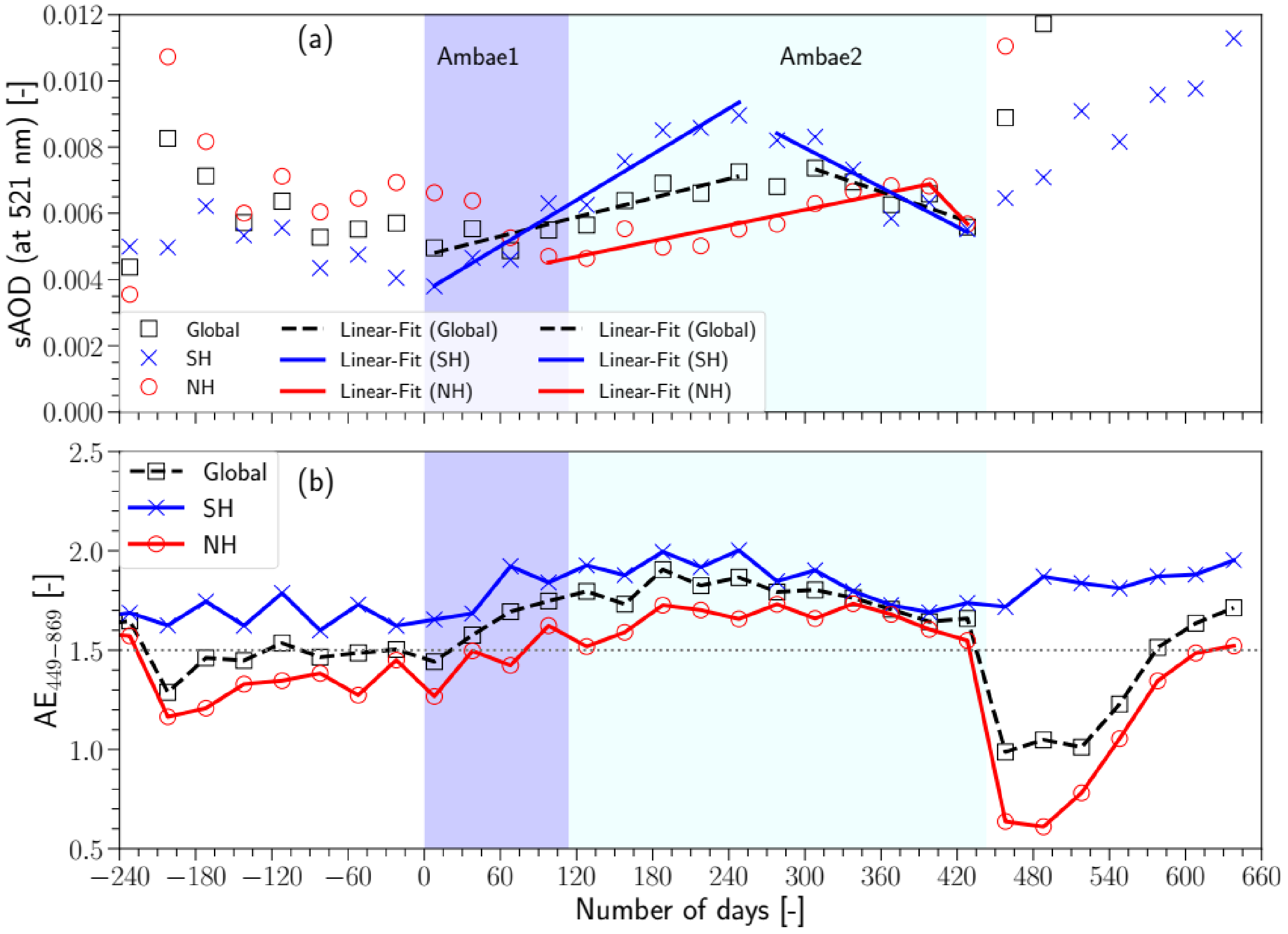

Dominance of small sulfate particles 🡐 $AE_{449\text{-}869} > 1.5$

- **Steep increasing slope** in the sAOD observed in the SH during the Amabe1 and Ambae2 periods (approx. 249 days)
- Although a similar increasing slope in the sAOD was observed for **Global** and **NH** regions, they have different starting and ending days in both regions, indicating a time lag existed with respect to the dispersion from SH to NH.
- Rate of decrease in sAOD is more drastic in NH than globally, with different starting days and the same ending day.
- Differences in the growth and decay periods of sAOD are characteristics of prevailing horizontal and vertical dispersion mechanisms in different regions.

Temporal Characteristics

sAOD corresponding to latitude bands depicted a similar pattern (with lower magnitudes) as represented by their respective extended regions (NH and SH).

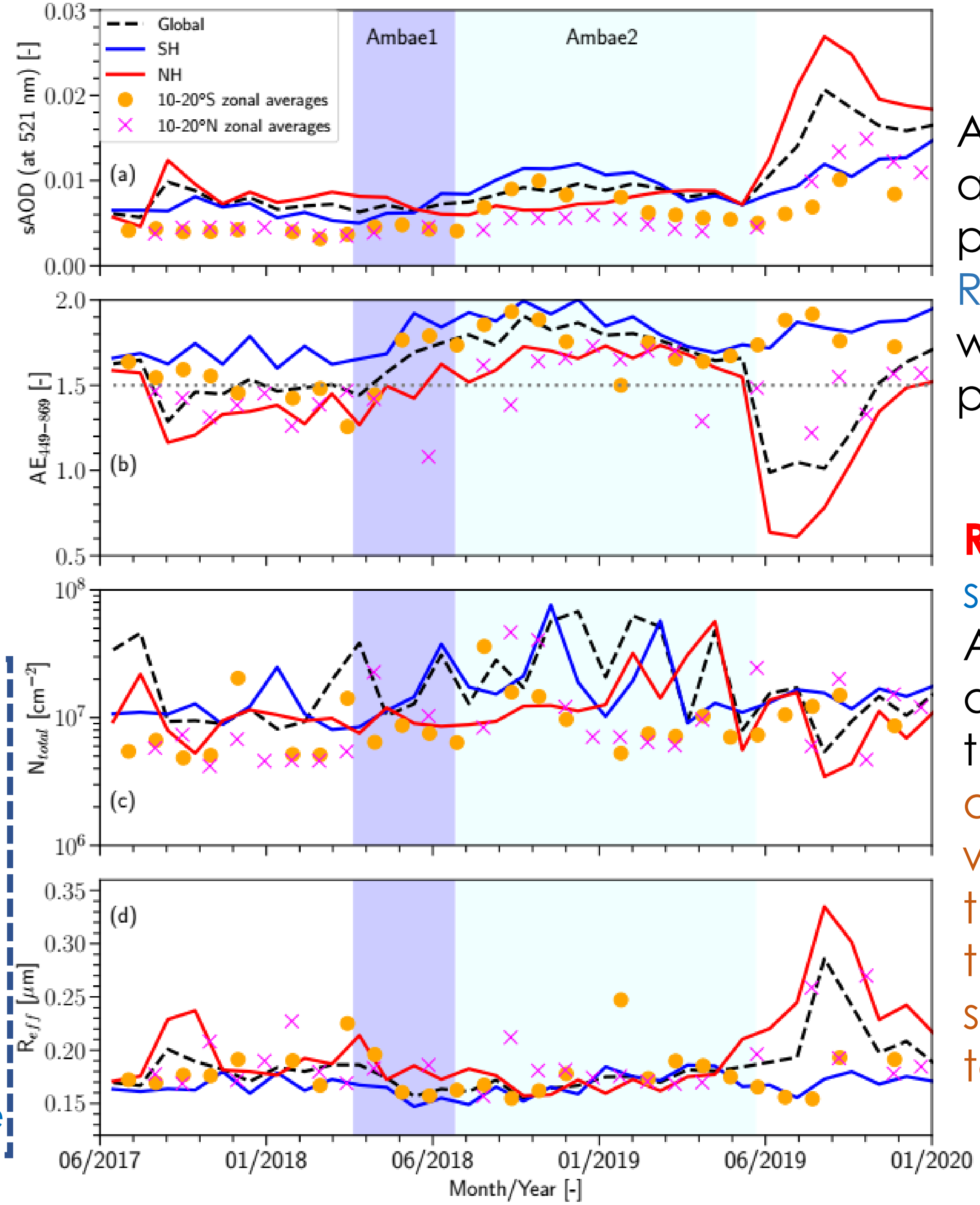

AE values were lowest (0.6 and above) during the post-Ambae period 🡐 Possible influence of Raikoke eruption (associated with comparatively larger ash particles)

Reff remained stable with no significant changes during pre-Ambae and Ambae periods in all regions, possibly because the microphysical changes associated with Ambae plume were not evidently visible in the derived **Reff** obtained from the number size distributions of spectral sAODs corresponding to an altitude range.

Strong fluctuations in N_{total}

- Temporal variation in the AE.
- Retrieval algorithm does not have any constraints for the temporal variation.
- Overestimation of fine mode

Radiative Impact

Volcano name	Eruption date(s) (dd/mm/yyyy)	Latitude	VEI	Estimated SO_2 loading (Tg)	Change in sAOD (-)	Estimated RF (W/m^2) TOA	Estimated RF (W/m^2) Surface
El Chichon [62,66,67] (El)	04/04/1982	17°N	5	7–12	0.10–0.14 (550 nm)	–2 to –4 (SW)	–
Nevado del Ruiz [67–69] (Ne)	14/11/1985	5°S	3	∼ 0.7	0.006 (550 nm)	–	–
Mt. Pinatubo [60,63,67,69,71] (Pi)	15/06/1991	15°N	6	20	0.15–0.20 (550 nm)	–4 to –5 (SW) –6 to –7 (LW)	– –
Kasatochi [1,72,74] (Ka)	07/08/2008	52°N	4	0.7–2.2	0.0023 (550 nm)	–2.1 (SW, all-sky) –0.04 to –2.0 (SW, clear-sky)	–
Sarychev [70,73,74] (Sv)	15/06/2009	48°N	4	1.2±0.2	0.005 (550 nm) ≈ 0.012	–0.16 (SW) –0.2±0.2 (SW)	–
Nabro [1,73,75,76] (Nb)	12–13/06/2011	13°N	4	1.3–2	≈ 0.09 (550 nm)	–1.03 (SW)	–
Ambae [30,31] (Am)	5–6/04/2018 27/07/2018	15°S	3	0.12 ≈ 0.36	0.007–0.009 (532 nm)	**–0.45** to **–0.6** (SW, Global) **–0.13** (SW, Tropics)	–
Raikoke [24] (Ra)	21–22/06/2019	48°N	4	1.5±0.2	≈ 0.025 (at 675 nm; NH)	**–0.27** to **–0.38** (SW, clear-sky) **–0.11** to **–0.16** (SW, all-sky)	–
Ulawun [24] (Ul)	26/06/2019 03/08/2019	5°S	4	0.14 0.30	0.010 (449 nm, Tropics)	**–0.09 to –0.13** (SW, clear-sky) **–0.04 to –0.05** (SW, all-sky)	–
Hunga Tonga-Hunga Ha-apai (HT) [42,77,78]	15/01/2022	20.6°S	5-6	0.4	∼ 0.22 (675 nm, Tropics) ∼ 0.15 (675 nm, SH)	**–0.6** (SW+LW; aerosol) **+0.8** (SW+LW; water vapor) **+0.2** (SW+LW; aerosol+water vapor)	**–1.7** (SW+LW; aerosol) **+0.0018** (SW+LW; water vapor) **–1.7** (SW+LW; aerosol+water vapor

Strongest climate impact for 2018

Conclusions

Based on the retrievals from inversion method

- Size distribution retrievals are strongly dependent on the choice of wavelengths, which in turn determine the shapes of the curves.
- Volume size distributions were found to manifest bi- and tri-modal shapes with distinct differences over each region at different time periods.
- Microphysical changes were not evidently visible through the derived R_{eff} as the number size distributions correspond to spectral sAOD values obtained for a fixed altitude range.
- Strong fluctuations in N_{total} can result because of temporal variation in AE and overestimation of the fine mode in the number size distributions.

Refer to:

https://doi.org/10.3390/rs15010029

Based on the retrievals from SAGE III/ISS observations

- Spectral dependency of sAOD values was found to be similar and lower in all regions during the pre-Ambae and Ambae1 periods.
- Influence of Raikoke eruption on sAOD values is significant (increased by 2-3 times) in NH, global, and 10 to 20° N latitudinal band.
- Ulawun eruption has a slight enhancement in sAOD values in SH and 10 to 20° S latitudinal band.
- Rate of change (growth/decay) in sAOD on a global scale resembled the changes in the SH, unlike the time lag associated with the changes in the NH.

Thank you ...